

## REVIEW ARTICLE

# Plastic structures for diverse substrates: A revisit of human ABC transporters

Wen-Tao Hou  | Da Xu | Liang Wang | Yu Chen | Zhi-Peng Chen |  
Cong-Zhao Zhou | Yuxing Chen

School of Life Sciences, University of Science and Technology of China, Hefei, People's Republic of China

## Correspondence

Cong-Zhao Zhou and Yuxing Chen, School of Life Sciences, University of Science and Technology of China, Hefei 230026, People's Republic of China.  
Email: [zcz@ustc.edu.cn](mailto:zcz@ustc.edu.cn) and [cyxing@ustc.edu.cn](mailto:cyxing@ustc.edu.cn)

## Funding information

the Strategic Priority Research Program of the Chinese Academy of Sciences, Grant/Award Number: XDB37020202; Fundamental Research Funds for the Central Universities, Grant/Award Numbers: YD9100002014, YD20700002005; Ministry of Science and Technology of the People's Republic of China, Grant/Award Numbers: 2020YFA0509302, 2019YFA0508500; National Natural Science Foundation of China, Grant/Award Number: 32071206

## Abstract

ATP-binding cassette (ABC) superfamily is one of the largest groups of primary active transporters that could be found in all kingdoms of life from bacteria to humans. In humans, ABC transporters can selectively transport a wide spectrum of substrates across membranes, thus playing a pivotal role in multiple physiological processes. In addition, due to the ability of exporting clinic therapeutics, some ABC transporters were originally termed multidrug resistance proteins. Increasing investigations of human ABC transporters in recent years have provided abundant information for elucidating their structural features, based on the structures at distinct states in a transport cycle. This review focuses on the recent progress in human ABC structural analyses, substrate binding specificities, and translocation mechanisms. We dedicate to summarize the common features of human ABC transporters in different subfamilies, and to discuss the possibility to apply the fast-developing techniques, such as cryogenic electron microscopy, and artificial intelligence-assisted structure prediction, for future studies.

## KEYWORDS

conformational dynamics, human ABC transporters, perspectives, structural feature, substrate binding specificity, translocation mechanism, transport cycle

## 1 | INTRODUCTION

ATP-binding cassette (ABC) transporters are ubiquitous transmembrane proteins, which participate in various biological processes through the transport of diverse substrates.<sup>1</sup> They are characterized by the nucleotide-binding domains (NBDs), which can bind and hydrolyze ATP, providing energy to transport the substrate(s) across the membrane. In total, there are 48 ABC members encoded by the human genome, which are divided into seven subfamilies from A to G (Figure 1A), based on the sequence homology.<sup>2</sup> However, members in the subfamilies ABCE and ABCF do not possess the transmembrane domains (TMDs), thus they are not bona fide transporters.

Due to participating in diverse physiological pathways, the malfunction of ABC transporters causes a variety of human diseases, such as intrahepatic cholestasis,<sup>3</sup> atherosclerosis,<sup>4</sup> X-linked adrenoleukodystrophy,<sup>5,6</sup> cystic

fibrosis,<sup>7,8</sup> retinal degenerations,<sup>9</sup> and sideroblastic anemia with ataxia (Figure 1B).<sup>10</sup> Notably, exogenous molecules, even anticancer chemicals, can also be transported as substrates because of the broad substrate spectrum of some ABC transporters, which thus become the notorious multidrug resistant proteins.<sup>11</sup> Therefore, the functional and structural studies of human ABC transporters have gained extraordinary attention in order to decipher their molecular mechanisms and pathogenesis.

Nowadays, structural information of at least one member is available for each subfamily of human ABC transporters. Based on the architectures and TMD sequence homology, all structure-known human ABC transporters belong to either type IV or type V ABC transporters.<sup>12</sup> Specifically, members from ABCB, ABCC, and ABCD subfamilies are type IVs, while those from ABCA and ABCG are type Vs. Both type IV and V ABC transporters exhibit the canonical architecture of ABC exporters consisting of two TMDs of 6 + 6

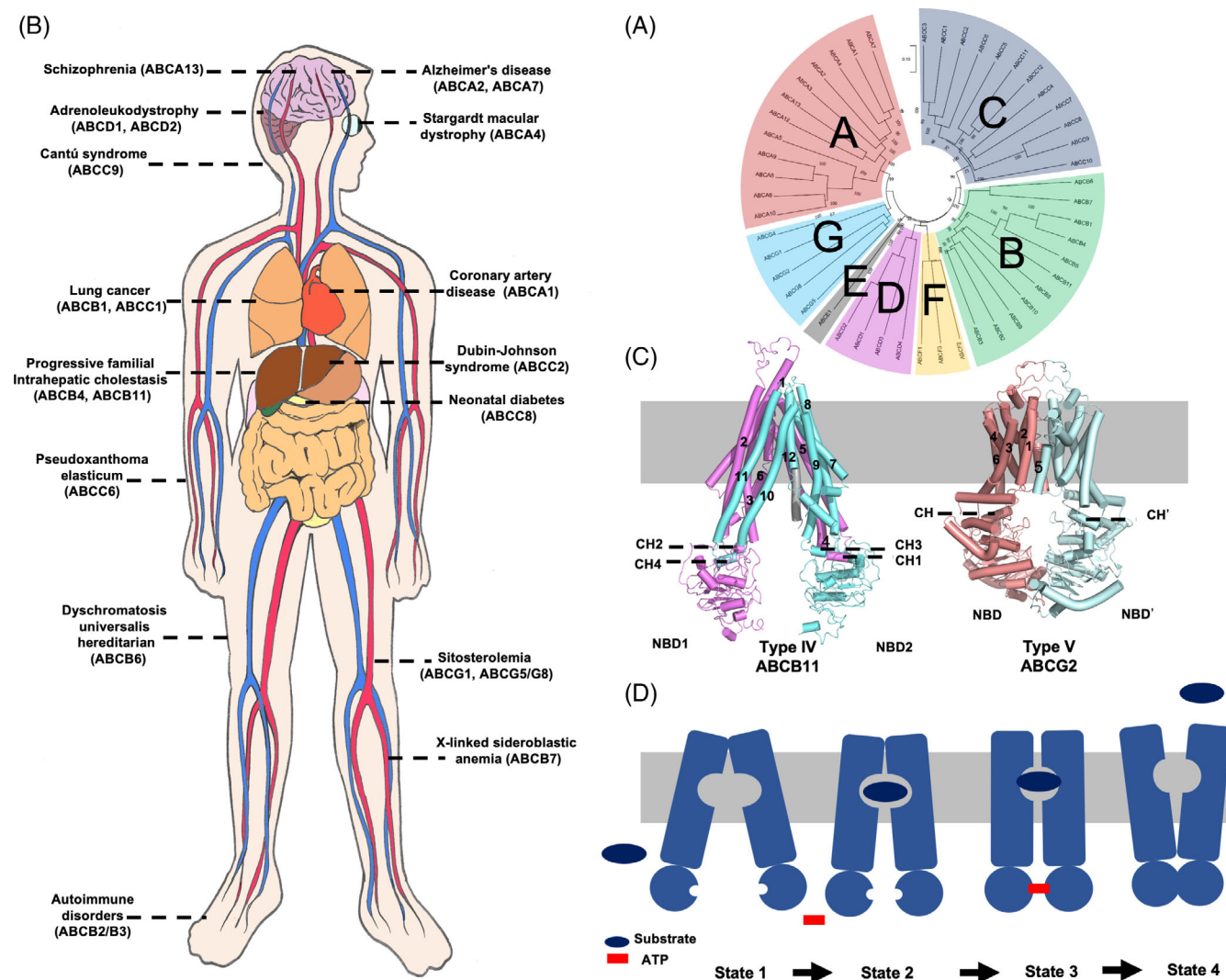


**FIGURE 1** Human ATP-binding cassette (ABC) transporters. (A) The phylogenetic tree of human ABC transporters of A to G subfamilies, which is produced by ClustalX2<sup>126</sup> and MEGA-X.<sup>127</sup> (B) Human diseases related to dysfunction of human ABC transporters. (C) Structural features of type IV and type V transporters. Apo-form structures of ABCB11 (PDB: 6LR0) and ABCG2 (PDB: 5NJ3) are shown as representatives. Two transmembrane domains (TMDs) are shown in different colors. The gray helix in ABCB11 is the interdomain linker. CH, coupling helix. (D) A scheme of the alternating access mechanism for ABC exporters. Nucleotide-binding domain (NBDs) and TMDs are indicated by a pair of ellipses and rectangles, respectively

transmembrane helices and two highly conserved NBDs, each of which contains an  $\alpha$ -helical subdomain and a RecA-like ATPase core subdomain.

In contrast, TMDs of IV and V types are quite different from each other. A type IV ABC transporter is featured with two cytosolic-extended TMDs, which dimerize via domain swapping (Figure 1C). Each protomer possesses two coupling helices lying in the interface between TMDs and NBDs, one formed by the TMs at the same protomer and the other by domain swapping TMs from the opposite TMD. Thanks to the extra TM extensions, the translocation cavity of type IV could become more widely open, allowing the access of substrates from either the intracellular or membrane lateral side depending on the chemical properties of substrates. In contrast, the type V ABC transporter possesses much shorter TMs (Figure 1C). Presumably, the

translocation cavity of type V is more likely with restricted access from the membrane, compared to type IVs, thus in most cases, the substrates enter the cavity via lateral access. For each protomer, only one coupling helix from TMD is embedded in the groove of the corresponding NBD.

For most ABC transporters, an alternating access mechanism is broadly accepted.<sup>12–14</sup> Taking ABCB1 as an example (Figure 1D): at the beginning of a transport cycle, the apo form adopts an inward-facing conformation<sup>15</sup> (State 1) wherein substrate could access from the cytosol, or laterally from the lipid bilayer. Once the substrate is bound, the transporter would convert to an occluded conformation or an inward-facing conformation with a narrowed transport cavity (State 2). Upon ATP binding, an occluded state where ATP and substrate are bound simultaneously exists for a short time, which was

first observed in the structure of the *Bacillus subtilis* transporter BmrA (State 3).<sup>16</sup> However, the dimerization of the NBDs would quickly trigger the conformational change to the outward-facing conformation, resulting in release of the substrate (State 4). Finally, hydrolysis of ATP drives the two NBDs apart and resets the transporter to the rest state (State 1). However, the alternating access mechanism can only roughly depict the major states of a transport cycle. A recent report of 16 structures of a heterodimeric ABC transporter TmrAB from *Thermus thermophilus* revealed multiple intermediate states in addition to the above four major states.<sup>17</sup>

Thanks to the technical development of cryogenic electron microscopy (cryo-EM) technology, there are rapidly increasing structures of human ABC transporters reported recently. To date, hundreds of structures of human ABC transporters are available in Protein Data Bank (PDB, <https://www.rcsb.org/>), which covers all subfamilies from A to G (the representative structures are listed in Tables 1 and 2). The accumulation of structures enables us to better understand the transport mechanisms and substrate specificities of ABC transporters. A series of previous reviews of ABC transporters in both biochemical and structural studies are available,<sup>12–14</sup> this review will mainly focus on human ABC transporters to summarize their characteristics from a structural perspective. We hope to delineate a horizon for future studies on human ABC transporters, and provide a structural platform for the development of therapeutic intervention for related human diseases.

## 2 | ABCA SUBFAMILY: LIPID TRANSPORTERS

The ABCA and ABCG subfamilies belong to type V ABC transporters, and are mostly involved in lipid metabolism. Specifically, ABCAs mainly participate in lipid trafficking, while many members of ABCGs play important roles in the transport of sterols.

ABCA subfamily contains 12 members (ABCA1–ABCA10, ABCA12, and ABCA13), which possess more residues than other subfamilies due to their large extracellular domains (ECDs). Among them, ABCA13 is the largest ABC transporter, which is composed of 5058 residues with an ECD of 3500 residues. It is suggested that the ECDs of ABCAs are important not only for substrate translocation, but also for interactions with protein partners.<sup>18</sup>

Till now, both structures of ABCA1 and ABCA4 are available in PDB (Table 1),<sup>18–21</sup> enabling us to take a glimpse of the common structural features of the ABCA subfamily. As type V transporters, they fold without TM swapping, featured with the ECDs, compared to the ABCG subfamily (Figure 2). ABCA1 mediates the lipid export and loading to apoA-I, which initiates the reverse cholesterol transport to prevent foam cell formation and atherosclerosis by clearing excess cholesterol from arterial vessels.<sup>22</sup> The structure of ABCA1 comprises two separately folded TMDs, a typical feature of the type V exporters. Each TMD contains six TMs with nearly no cytoplasmic extensions observed in the type IV exporters. The succeeding regulatory domains (R domain, or RD) may enhance the cooperativity between the two

halves of the ABCA1 transporter and modulate the transport activity. Each TMD of ABCA1 contains two transverse helices (IHs), preceding TM1 and between the TM2 and TM3, respectively, on the intracellular boundary of the membrane. The IHs between TM2 and TM3 extend more into the NBDs and can be recognized as the coupling helices, while the other pair could facilitate the crosstalk between the NBDs and the TMDs. In contrast, the coupling helices in type IV ABC exporters extend beyond the lipid bilayer into the cytoplasm, and are buried more deeply in the NBDs (Figure 1D). In this ABCA1 structure, all the other lateral surfaces of TMD1 and TMD2 are mostly exposed to the lipid bilayer (Figure 2A). Therefore, the lipid substrates from the inner leaflet of the membrane may still be able to access the substrate binding site in the seemingly “outward-facing” conformation. ECD1 in ABCA1 consists of 21  $\alpha$ -helices and 10  $\beta$ -strands, while the smaller ECD2 comprises 6  $\alpha$ -helices and 7  $\beta$ -sheets. The two ECDs are co-folded in a twisted manner, placing ECD1 largely above TMD2 and ECD2 on top of TMD1 (Figure 2A).<sup>20</sup> The flame-shaped ECD can be divided into three layers from the bottom to the top: the base, the tunnel, and the lid (Figure 2A). The base is co-constituted by both ECD1 and ECD2, each of which folds into an  $\alpha/\beta$  domain. Above the base, the tunnel is primarily formed by helices from ECD1 and an  $\alpha$ -helical hairpin from ECD2. The helical domains in ECD1 and ECD2 together enclose an elongated tunnel that is  $\sim 60$  Å in length and mostly hydrophobic. The lid, consisting of a small  $\alpha/\beta$  domain from ECD1, sits above the tunnel. It is notable that discontinuous densities can be observed tandemly lining up the tunnel in this structure, supporting a surmise that the tunnel may function as potentially temporary storage or delivery passage for lipids. The tunnel is open to the outside milieu on both the distal and proximal ends, while is accessible to solvent through a narrow aperture that would preclude the passage of lipids. At the proximal end, however, the opening is wide enough for lipids to pass through.

ABCA4 (also known as ABCR) is a retinal-specific ABC transporter, and is predominantly expressed in the outer segment disk membranes of photoreceptor cells. ABCA4 functions as a flippase to translocate N-retinylidene-phosphatidylethanolamine (N-Ret-PE), a reversible covalent adduct of all-trans-retinal (ATR) and phosphatidylethanolamine (PE), from the luminal leaflet to the cytoplasmic leaflet of the disk membrane.<sup>23–25</sup> After translocation, N-Ret-PE can be hydrolyzed to ATR and PE, thereby enabling ATR to be reduced to all-trans-retinol (ATRoI) by the cytoplasmic retinal dehydrogenase (RDH).<sup>26</sup> Thus, the toxic ATR in photoreceptor cells following photoexcitation is removed from the luminal leaflet of the disc membrane and then goes into the retinoid cycle for the regeneration of 11-cis-retinal.<sup>27,28</sup> Dysfunction of ABCA4 is related to the Stargardt disease, a most common heritable macular degenerative disorder,<sup>9</sup> and several other severe visual disorders, such as age-related macular degeneration,<sup>29</sup> retinitis pigmentosa,<sup>30</sup> and cone-rod dystrophy.<sup>31</sup>

A series of ABCA4 structures have been independently reported by three groups (Table 1).<sup>18,19,32</sup> The apo-form structure of ABCA4 shares most features with the previously reported ABCA1, while substrate-bound and ATP-bound ABCA4 structures supplement our knowledge of ABCA subfamily (Figure 2A).

**TABLE 1** Structures of type V human ABC transporters

Protein	Method and PDB ID	Conformation	Ligand
ABCA1	Cryo-EM; 5XJY <sup>20</sup>	Outward-facing	None
	Cryo-EM; 7TC0 <sup>21</sup>	Outward-facing	Cholesterol
	Cryo-EM; 7TBZ <sup>21</sup>	Outward-facing	Cholesterol
	Cryo-EM; 7TBY <sup>21</sup>	Outward-facing	Cholesterol
	Cryo-EM; 7TBW <sup>21</sup>	Occluded	ATP/cholesterol
ABCA3	Cryo-EM; 7W01 <sup>128</sup>	Lateral-opening/outward-facing	Lipid
	Cryo-EM; 7W02 <sup>128</sup>	Occluded	ATP
ABCA4	Cryo-EM; 7LKZ <sup>32</sup>	Occluded	ATP
	Cryo-EM; 7LKP <sup>32</sup>	Outward-facing	None
	Cryo-EM; 7E7O <sup>18</sup>	Outward-facing	N-ret-PE
	Cryo-EM; 7E7I <sup>18</sup>	Outward-facing	None
	Cryo-EM; 7E7Q <sup>18</sup>	Occluded	ATP
	Cryo-EM; 7M1P <sup>19</sup>	Outward-facing	None
	Cryo-EM; 7M1Q <sup>19</sup>	Outward-facing	N-ret-PE
ABCG1	Cryo-EM; 7OZ1 <sup>37</sup>	Inward-facing	ATP
	Cryo-EM; 7R8D <sup>36</sup>	Inward-facing	Cholesterol
	Cryo-EM; 7R8C <sup>36</sup>	Inward-facing	None
	Cryo-EM; 7R8E <sup>36</sup>	Outward-facing	ATP
	Cryo-EM; 7FDV <sup>38</sup>	Inward-facing	Cholesterol
ABCG2	Cryo-EM; 5NJ3 <sup>40</sup>	Inward-facing	None
	Cryo-EM; 6ETI <sup>41</sup>	Inward-facing	MZ29
	Cryo-EM; 6FFC <sup>41</sup>	Inward-facing	MZ29
	Cryo-EM; 6FEQ <sup>41</sup>	Inward-facing	MB136
	Cryo-EM; 6HCO <sup>42</sup>	Inward-facing	Estrone-3-sulfate
	Cryo-EM; 6HBU <sup>42</sup>	Outward-facing	ATP
	Cryo-EM; 6VXF <sup>43</sup>	Occluded/closed	None
	Cryo-EM; 6VXH <sup>43</sup>	Inward-facing	Imatinib
	Cryo-EM; 6VXI <sup>43</sup>	Inward-facing	Mitoxantrone
	Cryo-EM; 6VXJ <sup>43</sup>	Inward-facing	SN38
	Cryo-EM; 7NEZ <sup>44</sup>	Inward-facing	Topotecan
	Cryo-EM; 7NEQ <sup>44</sup>	Inward-facing	Tariquidar
	Cryo-EM; 7NFD <sup>44</sup>	Inward-facing	Mitoxantrone
	Cryo-EM; 7OJ8 <sup>45</sup>	Inward-facing	Estrone-3-sulfate/ATP
	Cryo-EM; 7OJH <sup>45</sup>	Inward-facing/more open conformation	Topotecan/ATP
Cryo-EM; 7JOI <sup>45</sup>	Inward-facing/more closed conformation	Topotecan/ATP	
ABCG5/G8	x-ray; 5DO7 <sup>48</sup>	Inward-facing	None
	Cryo-EM; 7R89 <sup>36</sup>	Inward-facing	Ergosterol
	Cryo-EM; 7R87 <sup>36</sup>	Inward-facing	None
	Cryo-EM; 7R88 <sup>36</sup>	Inward-facing	None
	Cryo-EM; 7R8B <sup>36</sup>	Inward-facing	Cholesterol

Interestingly, two substrate-bound ABCA4 structures displayed distinct poses of the substrate N-Ret-PE reported by two groups.<sup>18,19</sup> It is notable that the overall structures of the substrate-bound ABCA4 are essentially identical to the apo form based on the two studies. In the substrate-bound ABCA4 from Molday and colleagues (ABCA4-M),<sup>19</sup> N-Ret-PE was found to bind at the level of the

intradiscal (lumen) leaflet of the membrane and is accessible to the lipid bilayer. The N-Ret-PE substrate is wedged between TMD1 and TMD2 and capped with a loop (designated as the B-loop) from ECD1, but not observed in the structure of ABCA1. The  $\beta$ -ionone group of the retinal moiety is close to TM8 and TM11 and within a hydrophobic environment created by residues Ile1812, Leu1815, Leu1674,

**TABLE 2** Structures of type IV human ABC transporters

Protein	Method and PDB ID	Conformation	Ligand
ABCB1	Cryo-EM; 6C0V <sup>83</sup>	Outward-facing	None
	Cryo-EM; 6QEX <sup>84</sup>	Occluded	Taxol
	Cryo-EM; 6QEE <sup>84</sup>	Occluded	Zosuquidar
	Cryo-EM; 7A65 <sup>86</sup>	Occluded	None
	Cryo-EM; 7A69 <sup>86</sup>	Occluded	Vincristine
	Cryo-EM; 7A6E <sup>86</sup>	Occluded	Tariquidar
	Cryo-EM; 7A6F <sup>86</sup>	Occluded	Zosuquidar
	Cryo-EM; 7A6C <sup>86</sup>	Occluded	Elacridar
	Cryo-EM; 7O9W <sup>129</sup>	Occluded	Encequidar
ABCB2/B3	Cryo-EM; 5U1D <sup>123</sup>	Inward-facing	ICP47
ABCB4	Cryo-EM; 6SP7 <sup>130</sup>	Closed	None
	Cryo-EM; 7NIW <sup>131</sup>	Inward-open	Posaconazole
	Cryo-EM; 7NIV <sup>131</sup>	Occluded	Phosphatidylcholine
	Cryo-EM; 7NIU <sup>131</sup>	Apo-inward-open	None
ABCB6	Cryo-EM; 7D7R <sup>132</sup>	Inward-facing	None
	Cryo-EM; 7D7N <sup>132</sup>	Inward-facing	None
	Cryo-EM; 7EKL <sup>133</sup>	Occluded	None
	Cryo-EM; 7EKM <sup>133</sup>	Inward-facing	None
ABCB8	Cryo-EM; 7EHL <sup>134</sup>	Open-inward	None
ABCB10	X-ray; 4AYT <sup>135</sup>	Inward-facing	ACP
	X-ray; 3ZDQ <sup>135</sup>	Inward-facing	None
	X-ray; 4AYX <sup>135</sup>	Inward-facing	ACP
	X-ray; 4AYW <sup>135</sup>	Inward-facing	ANP
ABCB11	Cryo-EM; 6LR0 <sup>136</sup>	Inward-facing	None
	Cryo-EM; 7DV5 <sup>87</sup>	Inward-facing	Taurocholates
	Cryo-EM; 7E1A <sup>87</sup>	Inward-facing	Taurocholate
ABCC7	Cryo-EM; 6O2P <sup>113</sup>	Occluded	Ivacaftor
	Cryo-EM; 6O1V <sup>113</sup>	Occluded	GLPG1837
	Cryo-EM; 6MSM <sup>112</sup>	Occluded	ATP
	Cryo-EM; 5UAK <sup>111</sup>	Inward-facing	None
	Cryo-EM; 7SVR <sup>137</sup>	Inward-facing	Lumacaftor
	Cryo-EM; 7SVD <sup>137</sup>	Occluded	Lumacaftor
	Cryo-EM; 7SV7 <sup>137</sup>	Occluded	Tezacaftor
ABCC8	Cryo-EM; 6C3O <sup>117</sup>	Quatrefoil (NBD closed)	ATP/ADP
	Cryo-EM; 6C3P <sup>117</sup>	Propeller (NBD closed)	ATP/ADP
ABCD1	Cryo-EM; 7SHN <sup>138</sup>	Inward-facing	Oleoyl-CoA
	Cryo-EM; 7SHM <sup>138</sup>	Outward-facing	ATP
	Cryo-EM; 7RR9 <sup>139</sup>	Outward-facing	ATP
	Cryo-EM; 7RRA <sup>139</sup>	Inward-facing	None
	Cryo-EM; 7VWC <sup>67</sup>	Inward-facing	None
	Cryo-EM; 7VZB <sup>67</sup>	Inward-facing	Very long-chain fatty acid
	Cryo-EM; 7VX8 <sup>67</sup>	Outward-facing	ATP
ABCD4	Cryo-EM; 6JBJ <sup>71</sup>	Outward-facing	ATP

Ser1677, and Tyr345 from the B-loop. The retinal group is further stabilized through interactions with aromatic side chains of residues (Trp339, Tyr340, and Phe348) from the B-loop. Two positively charged arginine residues, Arg653 from TM2 and Arg587 from ECD1,

form salt bridges with the negatively charged phosphate group of N-Ret-PE. On the other hand, Gong and colleagues reported an N-Ret-PE molecule also completely exposed to the lipid bilayer,<sup>18</sup> but adopts a pose that sandwiched between the two TMDs in the luminal leaflet in



the substrate-bound ABCA4 (ABCA4-G). The retinol moiety and phosphate group are almost superimposed and recognized by the identical residues as in ABCA4-M (Figure 2A). However, the acyl chains of N-Ret-PE of ABCA-M are present within a hydrophobic environment created by TM1/2/7 in parallel with the membrane plane, remaining in contact with the lipid bilayer, while those from ABCA4-G extend toward the cytoplasmic space coordinated by TM1/2/5. The two structures are well consistent with a lateral access mechanism for the entry of substrates, and the retinol moiety and the phosphate group contribute largely to the substrate recognition.

In the ATP-bound structure of ABCA4, the cavity for binding N-Ret-PE is completely collapsed (Figure 2A). The transition between the nucleotide-free and ATP-bound conformations can be described as roughly rigid-body rotations of the two TMD-NBD-RD modules, TMD1-NBD1-RD1 and TMD2-NBD2-RD2, with almost no obvious structural change in the modules themselves. Both modules have rotated toward the molecular center to form the closed TMDs, and the more compact NBDs and RDs. The conformational changes are transduced to the ECDs, which exhibit an obvious rotation toward the membrane (Figure 2A).

### 3 | ABCG SUBFAMILY: CHOLESTEROL TRANSPORTERS

Structures of the ABCG subfamily are much simpler due to the absence of ECDs, compared to ABCAs (Figure 2), and prefer transporting smaller lipid molecules such as cholesterol. Five members of

the human ABCG subfamily have been identified, namely ABCG1, ABCG2, ABCG4, ABCG5, and ABCG8, which are half-transporters and thus function as homodimers or heterodimers.<sup>2</sup> It is worth noting that the ABCG subfamily transporters have a tandem organization from NBD to TMD, which are reversed in other human ABC transporters.

Subsequent studies showed that ABCG1 can promote the efflux of intracellular cholesterol to mature high-density and low-density lipoproteins (HDL and LDL), cyclodextrin, and liposomes; however, it could not present cholesterol to the lipid-free apoA-1 in the absence of ABCA1.<sup>4</sup> Previous studies indicated that *abca1*<sup>-/-</sup> mice accumulate a massive amount of neutral lipid in pulmonary macrophages, hepatocytes, and Kupffer cells, despite no lipid change can be detected in the plasma, while deficiency of *abca1* and *abcg1* in macrophage is sufficient to accelerate atherosclerosis in *ldlr*-knockout mice on a chow diet, suggesting the important role of ABCG1 in the reverse cholesterol transport.<sup>33-35</sup>

Recently, the Li group reported the high-resolution cryo-EM structures of human ABCG1 isoform 4 in apo-form, cholesterol-bound, and nucleotide-bound states (Table 1).<sup>36</sup> Moreover, the Locher group also reported a structure of cholesterol-bound ABCG1 isoform 4 at a resolution of 4 Å.<sup>37</sup> These structures provide a framework for an ABCG1-mediated cholesterol transport cycle, and identification of the cholesterol-binding sites. Residues Phe455, Met459, and Leu463 in TM2 and residues Phe555, Pro558, Val559, and Ile562 in TM5 of the other protomer engage the putative cholesterol substrate. They also observed a fatty acid chainlike density in the same cavity in the cholesterol-bound ABCG1<sub>EQ</sub>. Meanwhile, our group determined the

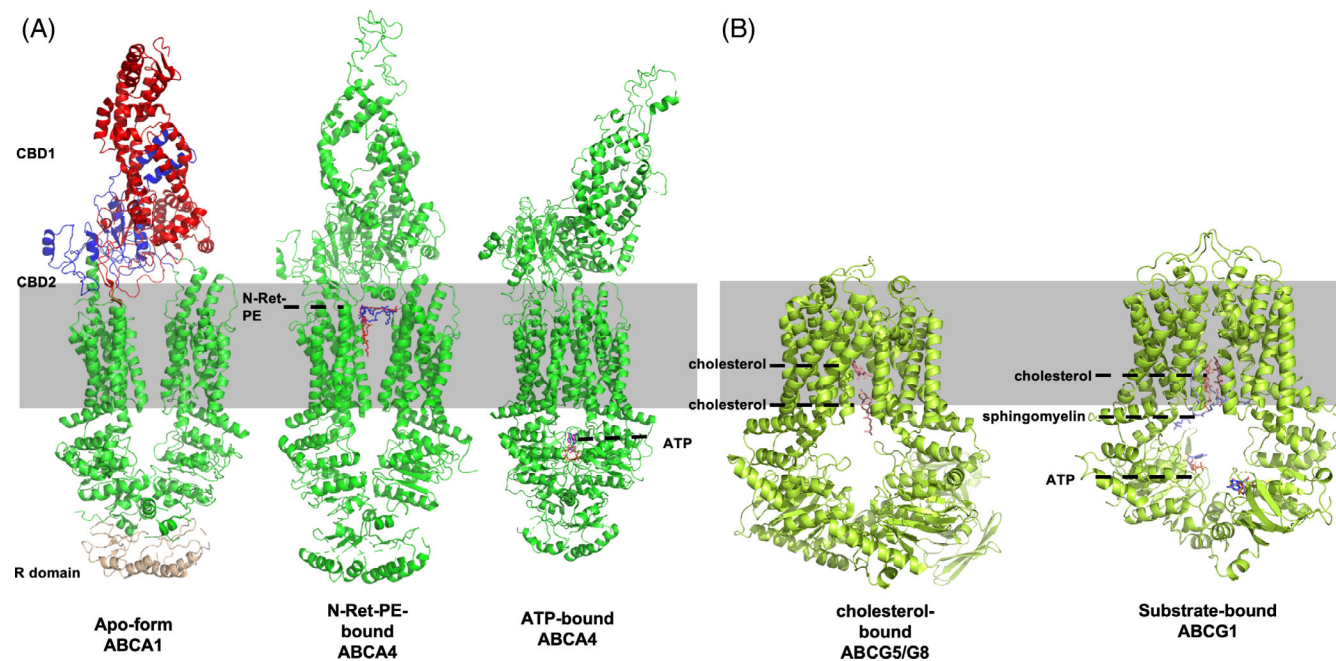


**FIGURE 2** Type V human ATP-binding cassette (ABC) transporters of ABCA and ABCG subfamilies. (A) Representative structures of ABCA subfamily. Different domains are colored in the apo-form of ABCA1 (PDB: 5XJY). Two molecules of N-Ret-PE are colored in red (from PDB: 7E7O) and blue (from PDB: 7M1Q), and the N-Ret-PE-bound ABCA4 structure of 7E7O is shown as the representative. (B) Representative structures of ABCG subfamily showing cholesterol-bound ABCG5/G8 (PDB: 7R8B) and substrate-bound ABCG1 (PDB: 7FDV)

structure of the canonical isoform 1 of the human ABCG1<sub>EQ</sub> in complex with cholesterol at a resolution of 3.26 Å by cryo-EM.<sup>38</sup> Structure-based functional analysis revealed not only an interaction network between ABCG1 and the substrate cholesterol, but also a phenylalanine-rich region approaching the exit of the substrate cavity, which is necessary for cholesterol efflux. Furthermore, we identified two sphingomyelin molecules bound to ABCG1, the densities of which were also observed by the Li group but failed in precise assignment most likely due to the relatively poor resolution. The sphingomyelin molecule also constitutes a part of the cholesterol-binding pocket (Figure 2B). Besides, our biochemical studies revealed that ABCG1 possesses an ATPase activity in a methyl-β-cyclodextrin stimulated manner in the presence of cholesterol. Altogether, it showed that both the cholesterol acceptor and the phospholipid sphingomyelin are critical for ABCG1-mediated cholesterol efflux.

ABCG2 is a constitutively expressed ABC transporter, whose physiological substrates include steroid derivatives and uric acid.<sup>39</sup> ABCG2 is also known as the breast cancer resistance protein, a multi-drug transporter that functions in many tissues including the mammary gland and the blood–brain, blood–testis, and maternal–fetal barriers. It also alters the pharmacokinetics of commonly used drugs and the delivery of therapeutics into tumor cells, thus leading to multi-drug resistance.

Since 2017, a series of studies have revealed structures of ABCG2 bound to substrates, nucleotides, small-molecule inhibitors, and antibodies (Table 1).<sup>40–46</sup> These structures provide different poses of ABCG2 in a substrate transport cycle, including the inward-facing apo form, the substrate-binding state, the transient states between the inward-facing and the outward-facing conformations, and the outward-facing ATP-binding state. Furthermore, the authors believed that the inhibitors make more interactions with ABCG2 compared to the substrates; moreover, the size of the substrates and inhibitors may determine which intermediate state is dominant in the transport cycle. They emphasized a plug formed by a pair of leucine residues of TM5, which separates the substrate-binding cavity and the external cavity in the TMD. In addition, Liao and colleagues revealed that ABCG2 might select its substrates by sensing whether the compound can effectively shift the initial apo-closed conformation to an inward-open state, and eventually transport the substrate via a closed-to-open switch pattern.<sup>43</sup>

The ABCG5/ABCG8 heterodimer (G5/G8) mediates the excretion of neutral sterols in the liver and intestines.<sup>47</sup> Mutations in G5/G8 cause sitosterolemia, a disorder characterized by sterol accumulation and premature atherosclerosis. The 3.9-Å crystal structure of the inward-facing conformation of the human ABCG5/8 complex is the first structure of ABCG transporters.<sup>48</sup> Besides basic features of a typical type V transporter, the two NBDs contact with each other at the distal cytoplasmic end to form a closed conformation through a pair of NPXDF motifs.<sup>41,46,49</sup> In addition, Li and colleagues reported the sterol-bound structures of ABCG5/G8 complex, which clearly revealed the sterol binding mode of ABCG5/G8.<sup>36</sup> One sterol molecule is bound within the cavity in the cytosolic leaflet (Site 1) between the TMDs of G5 and G8, adopting a pose in parallel with the TMDs.

The binding cavity is amphiphilic, with a negatively charged exit and a hydrophobic entrance. Moreover, another cholesterol binding site was discovered upon the addition of saturated cholesterol at 0.5 mM. The second cholesterol molecule is buried in a more hydrophobic cavity (Site 2) in the midway of the TMDs, and oriented in parallel to the membrane plane (Figure 2B). Similar to Site 1, one moiety of Site 2 is hydrophilic, comprising residues from TM2, TM5 of G5, and TM5 of G8; the other moiety is hydrophobic, formed by residues from TM1 and TM2 from G5, and TM5 from G8.

In summary, many fine mechanisms, such as the alternating-access mechanism for sterol substrate and whether the two substrates binding to the ABCG transporters could be transported during one single cycle, still remain unknown. Although sterol-binding Site 1 of ABCG5/G8 is similar in position to that of ABCG1, the factor that determines the difference in the cholesterol extrusion between them remains unclear, as ABCG1 cannot efflux intracellular cholesterol without extracellular cholesterol acceptor, whereas ABCG5/G8 complex can independently achieve the cholesterol transport into bile. Furthermore, the role of lipid in the functional regulation of membrane proteins, such as the sphingomyelin in ABCG1, is still enigmatic. Further experimental characterizations, as well as molecular dynamics simulations and single-molecule fluorescence, might be able to address these issues.

## 4 | ABCD SUBFAMILY: LIPID AND COBALAMIN TRANSPORTERS

In type IV transporters, ABCD subfamily members are also featured as lipid transporters, but are specifically involved in acyl-coenzyme A (CoA) esters transport. Human ABCD subfamily consists of four members: adrenoleukodystrophy protein (ALDP/ABCD1), ALDP-related protein (ALDRP/ABCD2), the 70-kDa peroxisomal membrane protein (PMP70/ABCD3), and the PMP70-related protein (P70R/ABCD4).<sup>5,50–52</sup> All members in ABCD subfamily are half-transporters. After being synthesized on cytosolic polysomes, ABCD1–3 are targeted to the peroxisome,<sup>52,53</sup> whereas ABCD4 is localized to the lysosome.<sup>54</sup> The N-terminal hydrophobic region seems to play an important role in the cellular localization of ABCDs. The N-termini of ABCD1 ~ 3 are captured selectively by PEX19, a protein that acts as both a cytosolic chaperone and an important receptor for peroxisomal membrane proteins, and then transported to the peroxisome.<sup>55,56</sup> However, the newly synthesized ABCD4 lacking the N-terminal hydrophobic region is first inserted into the endoplasmic reticulum and then translocated to the lysosome by interacting with the lysosomal membrane protein LMBD1.<sup>57</sup>

It has been indicated that ABCD1–3 transporters are involved in transporting acyl-CoA esters into the peroxisome.<sup>6,58–60</sup> Although their substrate specificities are partly overlapped, these three transporters show distinct substrate preferences. ABCD1 prefers to transport CoA esters of saturated very long chain fatty acid (VLCFA-CoAs), such as C24:0-CoA and C26:0-CoA.<sup>6,58,61</sup> Dysfunction of ABCD1 prevents VLCFAs from being transported into peroxisome for

$\beta$ -oxidation; thus causes X-linked adrenoleukodystrophy (X-ALD), a rare X-linked disease occurring in 1/20 000 males.<sup>62,63</sup> X-ALD is characterized by the accumulation of VLCFAs, particularly C24:0 and C26:0, in all human tissues.<sup>5,6</sup> X-ALD is a severe progressive, genetic disorder affecting the adrenal glands, the spinal cord, and the white matter (myelin) of the nervous system. X-ALD shows a wide range of phenotypes, and childhood cerebral adrenoleukodystrophy is the most common phenotype with the onset of neurological symptoms between 5 and 12 years of age, followed by rapidly processed central nervous system demyelination, and ultimately the death within a few years.<sup>62,63</sup> ABCD2, which shares a sequence identity of 62% with ABCD1, is capable of transporting most substrates of ABCD1, in addition to CoA esters of polyunsaturated fatty acids (PUFA-CoAs) such as C22:6-CoA and C24:6-CoA. Although there are no clinic case reports caused by the mutation in the ABCD2 gene, some studies suggested ABCD2 may play a role in docosahexaenoic acid metabolism.<sup>61,64,65</sup> ABCD3 shares 39% sequence identity with ABCD1 and specifically transport CoA esters of a dicarboxylic acid, branched-

chain fatty acid, and the bile acid intermediates di- and tri-hydroxycholestanoyl-CoA (DHCA and THCA). Congenital bile acid synthesis defect type V caused by ABCD3 mutations has been reported in one clinic case,<sup>66</sup> which suggests a critical role of ABCD3 in bile acid biosynthesis.

Recently, three ABCD1 structures at distinct states were determined by cryo-EM at atomic resolution, including the apo-form, the substrate- and ATP-bound structure (Figure 3).<sup>67</sup> In the apo-form state, ABCD1 adopts an inward-facing conformation, which is stabilized by the C-terminal coiled-coil helices. The TMDs exhibit a V-shaped lateral-opening conformation, allowing the entry of acyl-CoA from the cytoplasmic membrane leaflet. In the substrate-bound state, two C22:0-CoA molecules bind to two TMDs symmetrically and substrate-bound ABCD1 exhibits a narrower inward-facing conformation. For each C22:0-CoA, only the CoA portion enters the inward-facing cavity and lies in a positively charged pocket, whereas the acyl chain binds to the hydrophobic cleft formed by TM3 ~ TM6 from opposite TMD. Notably, this substrate

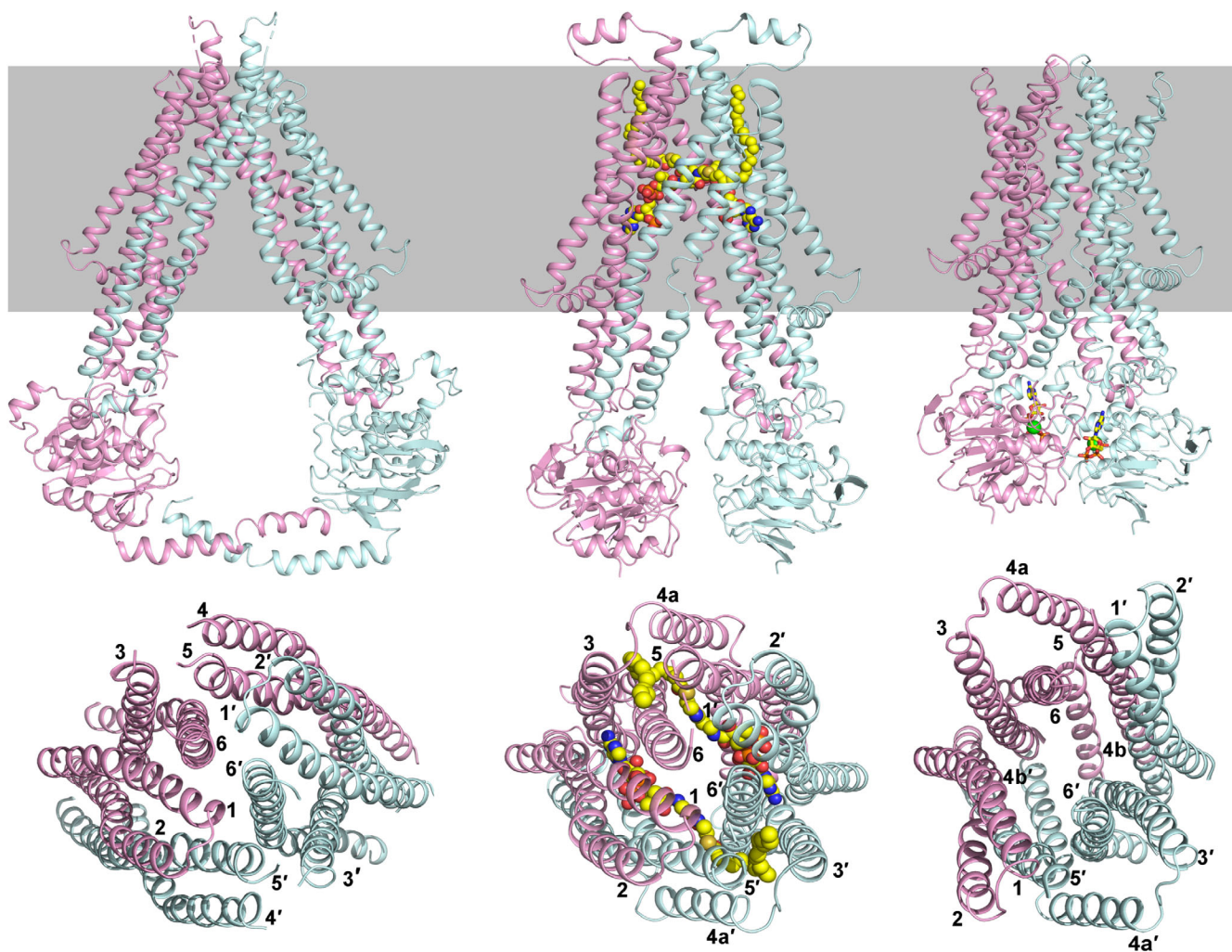


**FIGURE 3** Type IV human ATP-binding cassette (ABC) transporters of ABCD subfamilies. Three states of ABCD1 are shown as the representatives (PDB: 7VWC, 7VZB and 7VX8). TMs are numbered, and two protomers of ABCD1 are colored in pink and cyan, respectively. Two molecules of C22:0-CoA are shown as balls and ATP are shown in sticks, respectively



binding pattern is different from that adopted by all the previously known ABC transporters, in which the substrates are entirely located in a central cavity between the TMDs. Upon ATP binding, the dimerized NBDs make ABCD1 adopt an outward-facing conformation, ultimately facilitating the substrate release to the peroxisome matrix.

The conformational change between the substrate-bound and ATP-bound conformations can be described as a roughly rigid-body shifts of the TMs, resulting in an outward-facing conformation (Figure 3). Combined with the three structures obtained, we can find that all the TMs undergo rearrangement during these conformational changes (Figure 3). Viewed from the lumen of the peroxisome, the binding of substrate triggers relatively slight shifts of all TMs. TM1 and TM6 approach toward each other for binding CoA, while TM3, TM4, and TM5 shift inward for the binding of the acyl chain. The shift of these three TMs also leads to the interruption of TM4, in addition to the binding of cholesteryl hemi succinate Tris salt by the approached TM3 and TM4a. The two C22:0-CoA molecules are bound to two TMDs symmetrically, resembling two strings that “pull” the TMDs closer, resultantly generating a narrowed inward-facing conformation, accompanied by the closure of the translocation cavity at the cytosol side. Once ATPs are bound, the NBDs approach toward each other, and completely seal the translocation cavity. In consequence, TMs undergo great rearrangements as seen from the lumen of the peroxisome. Specifically, TM6 departs from TM1 and approach toward TM5, which also shifts away from TM3 and TM4, and finally sticks to TM1 of the other TMD. In addition, the two TM4b helices dimerize, and seal the translocation cavity from the cytosol side. These rearrangements lead to the opening of the cavity at the peroxisome matrix side, and enabling the release of acyl-CoA molecules. Combined with biochemical assays, these structures revealed a snapshot of the transport cycle of ABCD1. Although previous reports imply that ABCD1 possesses intrinsic thioesterase activity,<sup>68,69</sup> whether the acyl-CoA undergoes hydrolysis during the translocation process still cannot be determined solely based on the current structural information.

ABCD4 is indicated to transport cobalamin from the lysosomal lumen to the cytosol. In 2012, it was reported that mutations in the ABCD4 gene could cause a new inborn error of cobalamin metabolism with the phenotype of the failure to release cobalamin from lysosomes.<sup>54</sup> Recently, Imanaka and colleagues observed that ABCD4 is able to transport cobalamin from out of liposome in an ATPase activity-dependent manner,<sup>70</sup> which provided the first direct evidence that ABCD4 is capable of transporting cobalamin from the lysosomal lumen to the cytosol. The structure of ATP-bound ABCD4 has been determined previously.<sup>71</sup> As a type IV transporter, the overall structure of ABCD4 is very similar to ATP-bound ABCD1. However, ABCD1 transports substrates from the cytosol into the lumen of the peroxisome, while ABCD4 accepts cobalamin from the lysosomal lumen and exports it to cytosol. In 2020, the structure of AMP-PNP-hound Rv1819c, a homolog of ABCD4 from *Mycobacterium tuberculosis* was determined.<sup>72</sup> This structure exhibits an occluded conformation and forms a large hydrophilic cavity with

a volume of more than 7700 Å<sup>3</sup> much large than the volume of cobalamin, which is suggested to be a cobalamin binding pocket with low substrate specificity. To date, the hypothesis that ABCD4 transports cobalamin from lysosome lumen to cytosol has been supported by several lines of evidence, but the exact mechanism that how cobalamin is translocated remains obscure, and the structure of cobalamin-bound ABCD4 seems to be very direct evidence to be expected.

## 5 | ABCB SUBFAMILY: TRANSPORTERS OF DIVERSE SUBSTRATES AND RELATED TO MDR

TMDs of type V ABC transporters have longer extensions away from the membrane bilayers, resulting in a longer translocation cavity protruding into the cytoplasm (Figure 4A). This longer cavity makes it possible to accommodate various substrates, including hydrophilic, hydrophobic, and amphiphilic molecules, most likely via multiple routes to the cavity. Indeed, the type IV ABC transporters seem to possess a much broader spectrum of substrates compared to the type V. In fact, transporters in ABCB and ABCC subfamily have both been first discovered as multidrug exporters, thus initially referred to as multidrug-resistant (MDR) proteins<sup>11</sup> and multidrug resistance proteins (MRPs),<sup>73</sup> respectively.

Human ABCB subfamily consists of 11 members, which are named from ABCB1 to ABCB11. Four of them (ABCB1, ABCB4, ABCB5, and ABCB11) are full-transporters, and the rest are half-transporters. It is the only human ABC subfamily that possesses both full- and half-transporters. Because their functions are related to MDR or transport associated with antigen processing (TAP), it is also termed the MDR/TAP subfamily,<sup>74</sup> as seen from the greatly variable functions of this subfamily.

ABCB1 (P-gp/MDR1) is the first identified human ABC transporter,<sup>11</sup> which is responsible for the excretion of many endogenous and exogenous poisonous compounds. It can also pump many drugs out of cells and is well known for its ability to confer multidrug resistance to cancer cells, making ABCB1 a very promising drug target for cancer treatment.<sup>75,76</sup> Both ABCB2 (TAP1) and ABCB3 (TAP2) are involved in the adaptive immunity. The heterodimers ABCB2/B3 are localized on the endoplasmic reticulum to transport degraded peptides from cytoplasm to the endoplasmic reticulum, which might be presented as antigens by the major histocompatibility complex class I.<sup>77</sup> The phospholipid transporter ABCB4 (MDR3) and bile salts exporter ABCB11 (BSEP) are involved in bile secretion from hepatocytes to canaliculi, which are both localized on the apical membrane of hepatocytes.<sup>78</sup> Mutations of either ABCB4 or ABCB11 transporter are associated with various forms of progressive familial intrahepatic cholestasis (PFIC). For instance, mutations in the ABCB4 gene are related to PFIC3, resulting in defective flipping of phosphatidylcholine across the canaliculus.<sup>79</sup> Mutations in the ABCB11 gene may block the transport of bile salts into bile, causing PFIC2, which is the most severe cholestasis in all

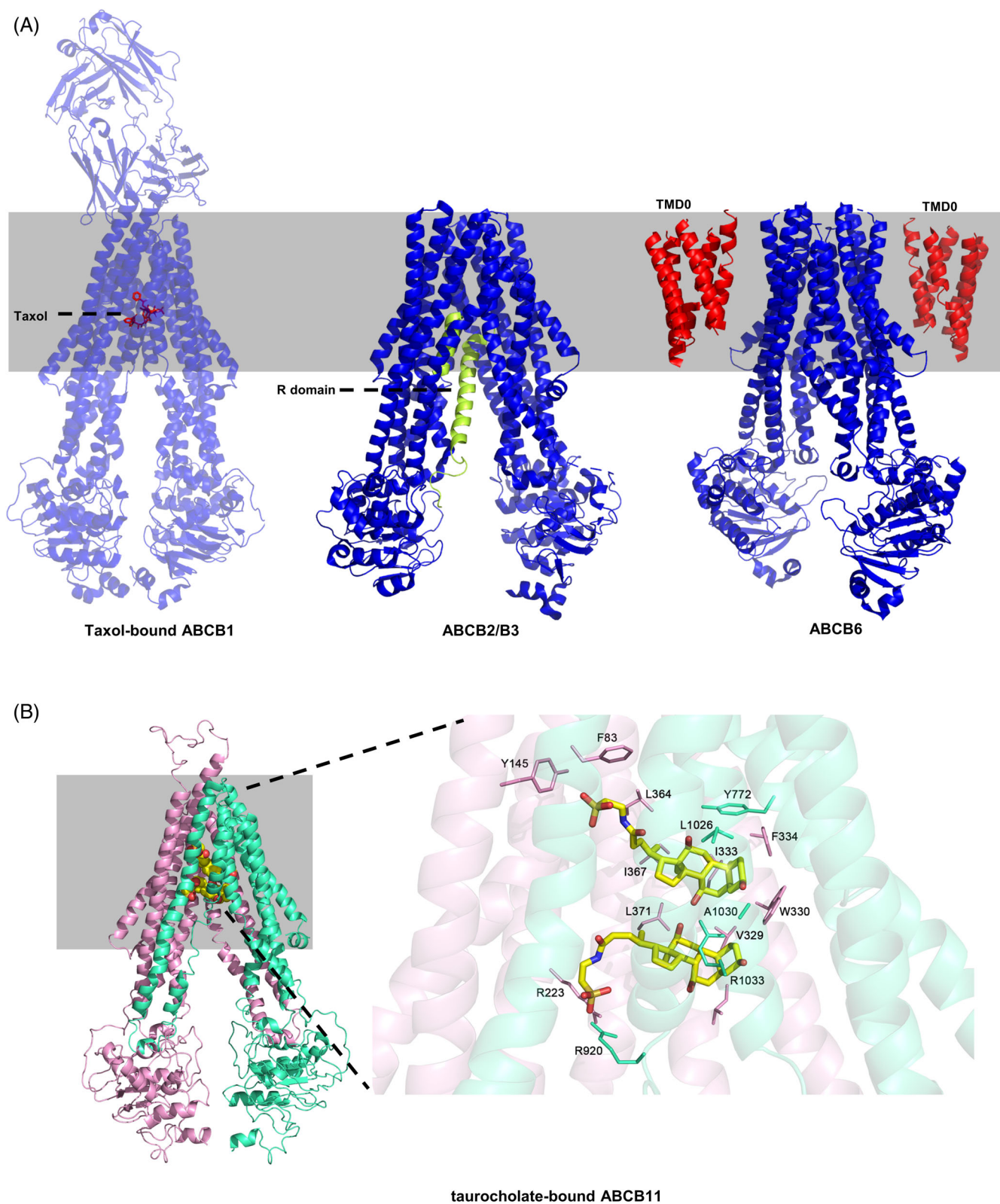


**FIGURE 4** Type IV human ATP-binding cassette (ABC) transporters of ABCB subfamilies. (A) Representative structures of ABCB subfamily showing Taxol-bound ABCB1 (PDB: 6QEX), ABCB2/B3 (PDB: 5U1D) and ABCB6 (PDB: 7D7R). (B) Two substrate-binding pockets in ABCB11 (PDB: 7DV5)

types of PFICs.<sup>3</sup> ABCB5 and antigen processing-like transporter ABCB9 have also been found to mediate multidrug resistance in

diverse malignant tumors.<sup>80,81</sup> The four half-transporters, ABCB6, ABCB7, ABCB8, and ABCB10 are localized to the outer (ABCB6) or

inner membrane (ABCB7, ABCB8, and ABCB10) of mitochondria, playing an important role in iron metabolism and transport of iron/thionine precursors.<sup>10</sup>

To date, except for ABCB5, ABCB7, and ABCB9, high-resolution structures of all other members in human ABCB subfamily have been solved by either x-ray crystallography or cryo-EM technology (Table 2). In addition, a homolog of ABCB7 from *Saccharomyces cerevisiae* has been solved.<sup>82</sup> Thus, only two members in B subfamily (ABCB5 and ABCB9) are structure-unknown. Structurally, all members of B subfamily belong to type IV ABC transporters.<sup>12</sup> In addition to the basic and core characteristics of type IV transporters, the heterodimer ABCB2/B3 contains two extra N-terminal TMD0 with four transmembrane helices of each; the homodimer ABCB6 harbors two extra N-terminal TMD0 with five transmembrane helices of each (Figure 4A). However, the exact functions of TMD0 remain unclear, despite it was suggested that TMD0 could help ABC transporter to be accurately localized or acts as a module to interact with other protein partners.

Notably, the structures of ABCB1 have been solved in multiple conformational states (Table 2), from which researchers elaborate the entire transport cycle from the initial inward-facing state ready for substrate binding to the outward-facing state for substrates release.<sup>83,84</sup> Specifically, the structures of ABCB1 bound with various substrates or inhibitors depicted a universal binding pattern, providing hints for the development of potent and more selective ABCB1 inhibitors. The first substrate-bound ABCB1 structure revealed a central, occluded pocket bound with taxol/paclitaxel, which is a chemotherapeutic compound (Figure 4A).<sup>84</sup> The pocket is formed by the closing of a gate region consisting of TM4 and TM10. All 12 TMs provide residues, which were clearly assigned in structure, contribute to the binding of taxol. However, the density of taxol is not clear, indicating the possibility of its multiple binding modes. Compared to the previously determined inward-open structures of mouse ABCB1, the NBDs adopt a conformation closer to each other. The results showed that the binding of taxol induces an occluded conformation and a concomitant closing of the inter-NBD gap. The boundary to determine a ligand whether the substrate or the inhibitor might be very subtle. For example, the inhibitors of ABCB1 as tariquidar and elacridar could also be transported as substrates at low concentrations.<sup>85</sup> Abundant structural information of inhibitor-bound ABCB1 unraveled the underlying inhibiting mechanisms.<sup>84,86</sup> Based on vincristine-, elacridar-, tariquidar-, and zosuquidar-bound ABCB1 structures (Table 2), two inhibitory modes were proposed<sup>15</sup>: one involves in full occupation and strong interaction with the substrate-binding pocket, as for vincristine; the other is to inhibit the transporter by tight binding of a second inhibitor molecule which extends from the substrate-binding pocket and binds to extra areas. The second mode explains why inhibitors could be transported as substrates at lower concentrations.

Unlike those with a single binding pocket at the central cavity, the full-transporter ABCB11 is the only human ABC transporter of known structure that possesses two asymmetric substrate-binding pockets in its TMD.<sup>87</sup> Specifically, the complex structures revealed that two taurocholate molecules are positioned within two semi-

connected substrate-binding pockets that are respectively located in the outer and inner membrane leaflets (OML and IML) of ABCB11s TMDs (Figure 4B). The hydrophilic moiety of TC is recognized by the OML pocket, whereas the hydrophobic moiety is well accommodated in the IML pocket. Extensive mutational follow-up studies in combination with diverse biochemical assays of monitoring ATPase and transport activities revealed that ABCB11 combines two distinct mechanisms for unidirectional transport of its amphipathic TC substrate across the membrane: (i) the anticipated ATP-mediated pumping out of substrate, but also (ii) a pocket-to-pocket transfer cascade that is driven by increasing substrate binding affinities. The second mechanism strongly resembles the long-known “facilitated diffusion” process, but which is unprecedented for previous structure-known ABC transporters.

In light of multiple-sequence alignment indicating that members of ABCB subfamily share high sequence similarity, each of them possesses a unique substrate specificity and transport mechanism. Although plentiful structures have been captured for each protein in the ABCB subfamily, the specified transport cycle and substrate recognition mechanism still remain unclear. For example, the sequence of ABCB1 shares 76% identity with ABCB4, but the former encodes a MRP and the latter devotes to lipid transport. While in the cases of ABCB7 and ABCB10, they prefer distinct substrates, but display an overlapped substrate specificity toward the same compound for Fe/S cluster synthesis in the cytosol.<sup>88</sup> Hence, it still is needed to crack the code of the substrate specificity of ABCB subfamily, which might make it possible to modify or artificially engineering the substrates specificity.

## 6 | ABCC SUBFAMILY: MRP AND CHANNEL RELATED

ABCC subfamily is frequently described as MRPs. In total, 9 out of 12 members have the ability to extrude anticancer drugs or xenobiotics out of the cell, except for ABCC7, ABCC8, and ABCC9.<sup>89–91</sup> Besides drugs, previous investigations have established that these MRPs are capable to efflux physiological anions, such as leukotriene C4, bilirubin, steroid hormone, and cyclic nucleotides and prostaglandin. In addition, glutathione (GSH), sulfate, or glucuronate conjugated molecules were also reported to be most likely transported by MRPs.<sup>92,93</sup>

ABCC1 is expressed in various tissues, including tumor cells. It is the most well studied MRP due to its ability to efflux anticancer drugs such as vinca alkaloids, methotrexate, mitoxantrone, camptothecins, anthracyclines, and saquinavir.<sup>74,94–96</sup> ABCC2 and ABCC3 share 50% and 58% sequence identities with ABCC1, respectively, and they also have an overlapped substrate specificity toward the anticancer drugs against ABCC1. However, unlike ABCC1, the physiological substrates of ABCC2 and ABCC3 have been identified. ABCC2 is located in the apical (canalicular) hepatocyte plasma membrane, small intestine, and renal proximal tubules, and is involved in bilirubin efflux from hepatocytes to canaliculi.<sup>90</sup> ABCC2 loss-of-function causes an inherited



disorder of bilirubin named as Dubin-Johnson syndrome.<sup>97</sup> ABCC3 can efflux organic anions into sinusoidal blood, including bilirubin, bile, DHEAS, MTX.<sup>98-100</sup> Unlike ABCC1-3, ABCC4 and ABCC5 displayed an obvious preference toward nucleotide and analog drugs,<sup>91,101</sup> such as 6-thioguanine, 6-mercaptopurine, and topotecan.<sup>92</sup> Moreover, ABCC4 is also reported to transport prostaglandin, bile acid, and urate, while ABCC5 has a high affinity toward cGMP and cAMP.<sup>91</sup> Other MRPs, namely ABCC6, ABCC10, ABCC11, and ABCC12 show similar substrate specificities as ABCC1, which are also involved in drug resistance during the chemotherapy with the ability to efflux anticancer drugs, antimetabolites, and organic anions.<sup>102</sup> Although no structure of human MRPs has been solved till now (Table 2), the structure of the ABCC1 homolog from *Bos taurus* at three states has been reported: the apo-form, leukotriene C4-bound, and ATP-bound.<sup>103,104</sup> These structures provide structural hints for human ABCC1 broad-spectrum amphiphilic substrates.

The other members, namely ABCC7, ABCC8, and ABCC9 are not involved with drug resistance. ABCC7, also known as cystic fibrosis transmembrane conductance regulator (CFTR), is a chloride channel located in epithelial cells. Mutations of the CFTR gene lead

to cystic fibrosis, a lethal genetic disease in populations of Northern European descents.<sup>7,8</sup> Studies have consistently shown that dysfunction of CFTR disturbs salt homeostasis in lung epithelial cells, the main clinical manifestations of which are mucus accumulation, recurrent pulmonary infections, and chronic inflammation.<sup>105</sup> ABCC8 and ABCC9, also known as the sulfonylurea receptors SUR1 and SUR2, respectively, function as the regulators of the inwardly rectifying potassium (Kir) channel.<sup>106</sup> SUR1 can regulate the potassium efflux of Kir6 by sensing the intracellular ADP/ATP ratio of pancreatic  $\beta$ -cells.<sup>107,108</sup> From solved cryo-EM structures, SUR and Kir6 are assembled into a hetero-octamer, named ATP-sensitive potassium ( $K_{ATP}$ ) channels, which play pivotal roles in insulin secretion in response to glucose level and sulfonylurea drugs (Figure 5A).<sup>109</sup> As a subunit of  $K_{ATP}$ , SUR2 is located in neurons, astrocytes, microglia, and vascular smooth muscle. Mutations of the SUR2 usually lead to sleep disorders and depression.<sup>110</sup>

In the structure of CFTR, the linker between NBD1 and TMD2 is also called the R (regulatory) domain, unlike R domains in ABCA subfamily that cover both N and C-termini. This dephosphorylated R domain occupies the central channel between the two TMDs and

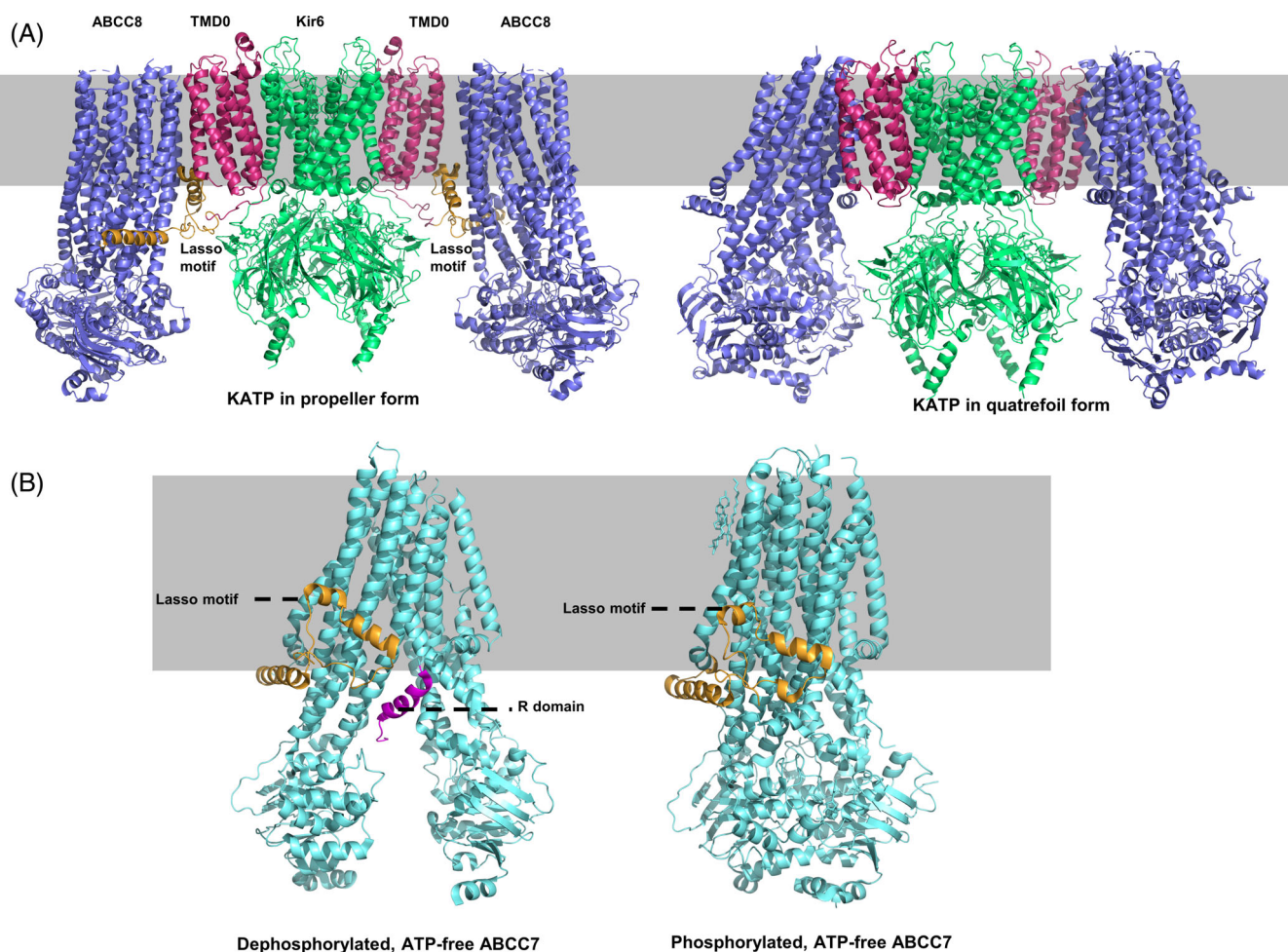


**FIGURE 5** Type IV human ATP-binding cassette (ABC) transporters of ABCC subfamilies. (A) Structures of KATP in two forms (PDB: 6C3O and 6C3P). (B) Structures of ABCC7 in two states (PDB: 5UAK and 6MSM)



prevents NBD dimerization (Figure 5B).<sup>111</sup> Upon phosphorylation, the R domain will be ejected from the central channel, which eventually promotes the dimerization of NBD.<sup>112</sup> Thus in the phosphorylated state, the density of the R domain is not observed in cryo-EM map (Figure 5B). Recently, CFTR structures complexed with two therapeutic compounds (ivacaftor and GLPG1837) have been resolved.<sup>113</sup> The two drugs bind to the TMDs of CFTR, inserting into a pocket formed by TM4, 5, and 8, and stabilize CFTR in the inward-facing configuration.

Structural information of human CFTR, and SUR1, as well as ABCC1 homolog from *B. taurus*, provides general structural features of the ABCC subfamily. All members of C subfamilies could be classified into type IV ABC transporters, with a highly conserved lasso motif.<sup>12,104</sup> In addition, the N-terminal TMD0 has been found in ABCC1-ABCC3, ABCC6-ABCC9. Previous studies have noted the importance of TMD0 in protein interaction.<sup>114-116</sup> TMD0 consists of five TMs, but the function of TMD0 remains a paucity of evidence. However, the SUR1 structure indicates that TMD0 provides an interactive interface for Kir6.<sup>117</sup> The Kir6 tetramer forms a central potassium ion channel, and the surrounding SUR1 binds to Kir6 through TMD0 (Figure 5A). In the structure of sulfonylurea-bound SUR1 homolog from *Mesocricetus auratus*, it has been found that sulfonylurea drugs stabilize the N-terminus of Kir6 via binding to SUR1, preventing the dimerization of NBDs.<sup>118</sup> In the absence of sulfonylurea drugs, the N-terminus of Kir6 binds to the SUR1 pocket at a lower affinity.<sup>119</sup>

Most members of the ABCC subfamily can transport anticancer drugs, displaying overlapped substrate specificities, but no structural information has been obtained to illustrate the underlying mechanisms. Moreover, ABCC1 and ABCB1 displayed overlapped substrate specificities toward drugs, including vinca alkaloids.<sup>94,96,120</sup> However, compared to plentiful structural studies of the ABCB subfamily, the information for MRPs is scarce, as no substrate or inhibitor-bound structures have been reported to date. It obstructs the development of new anticancer drugs to evade the efflux of MRPs, or the design of inhibitors that block the efflux of current drugs. In addition, the physiological conditions that enable us to capture the protein at the occluded state of ABCC7 remain unknown.

## 7 | CONCLUSION

We have depicted each subfamily of human ABC transporters in this review. Despite their functional diversity, the structure features make it possible to perfectly categorized them into type IV and type V transporters, respectively. However, unique structural features have evolved to execute diverse functions. Some of the unique features can be found in both types. For example, the R domain at the C-terminus of ABCA1 (type V) resembles highly the R domain (the C-terminal helices) in ABCD1 (type IV), which might play a similar role in enhancing the cooperativity between the two halves of NBDs. In addition, TMD0 has been found in both ABCB and ABCC subfamilies; and thus, the function of TMD0 in ABCB6 might be deduced from the

structures of ABCC8. The R domains located at the translocation cavity, either formed by the N-terminus in the case of ABCB2/3, or by the interdomain linker in ABCB11, might all interfere with the entrance of substrates, as revealed by the structures of ABCC7. Extracellular structural components, either as large as ECDs in the ABCA subfamily, or a pair of short helices in ABCD1, are proposed to be involved in facilitating the substrate release. These structural elements have been found among different subfamilies and displayed similar functions, revealing the convergent evolution of ABC transporters.

## 8 | PERSPECTIVES

### 8.1 | AI-assisted structural prediction

The development of cryo-EM has accelerated the accumulation of ABC transporter structural information. Moreover, the structural prediction breakthrough by AlphaFold-2 has pushed structural biology into a new era.<sup>121,122</sup> However, several shortcomings of protein structure prediction are nonnegotiable, limiting its substitutions of real structural determination. (1) It is still not accurate to predict the structures that no structural information of homologs is available. (2) Multiple and/or subtle conformational changes cannot be predicted, which is a special challenge for ABC transporters. (3) Though great breakthroughs have been achieved, the accuracy of structure prediction still cannot satisfy the precise drug design and iterated optimization. (4) The output of prediction tends to fit the present structural information, which might become an intrinsic bias. For example, the R-domain of ABCB11 has been predicted to be folded by the N-terminus, as revealed by the structures of ABCB2/B3<sup>123</sup> or an ABCB1 homolog.<sup>124</sup> However, from our bona fide structure of ABCB11, the R domain is actually folded by the interdomain linker, which is further confirmed by the structure of the N-terminus truncation version of ABCB11.<sup>87</sup>

### 8.2 | In situ structural determination

Despite all mentioned above, one should also keep in mind that structural information obtained by cryo-EM is the averaging of massive particles, which precludes the information of local inherent flexibility. More importantly, the preparation of cryo-EM specimens makes it difficult to maintain the natural state of ABC transporters. Despite the resolution being still limited, electron cryotomography (cryo-ET) seems to be the next revolution in the structural study of ABC transporters, as it can investigate the in situ structures of proteins.

### 8.3 | In vivo functional analysis and clinical interpretation

Varieties of functional analysis methods have been employed for the study of ABC transporters, such as the ATPase activity assays,

proteoliposome-based transport activity assays, and single-molecule fluorescence resonance energy transfer (or smFRET). The smFRET is a biophysical technique used to measure distances at the 1–10 nm scale in a single molecule, which is suitable for the study of conformational changes during a transport cycle. Although in vivo analysis has been widely used to study the function of ABC transporters, the complex intracellular microenvironment hampered a direct readout. Therefore, it is demanding to develop an in situ analysis platform at the single molecule level for the revolutionary study of ABC transporters, resembling the high-resolution cryo-ET.

In addition, the structures of ABC transporters also enable us to precisely map the known mutations and the related pathogenesis. For instance, a polymorphism in exon 13 of ABCB11 (V444A), which is associated with decreased hepatic BSEP expression is significantly more frequent in patients with drug-induced cholestasis, compared to the drug-induced hepatocellular injury patients and healthy controls.<sup>125</sup> The structural information indicates that this polymorphic site locates between A-loop and P-loop in the NBD, giving some hints for the therapeutic intervention and rational drug design.

Although a series of questions remain for ABC transporters, we could imagine cryo-EM and/or cryo-ET used to resolve dozens of structural conformations of a dynamic protein, or to discern the amino acid sequence of unknown components of a multiprotein complex, with the help of other biophysical, biochemical methods combined with structure predictions. These cutting-edge technologies will deepen our understanding of these crucial ABC complexes as well as related molecular machinery, which will promote future clinical and medicinal applications.

## ACKNOWLEDGMENTS

This work is supported by the Ministry of Science and Technology of China (2020YFA0509302, 2019YFA0508500), National Natural Science Foundation of China (32071206), the Fundamental Research Funds for the Central Universities (YD9100002014, YD20700002005), and the Strategic Priority Research Program of the Chinese Academy of Sciences (XDB37020202).

## ORCID

Wen-Tao Hou  <https://orcid.org/0000-0003-1762-1607>

## REFERENCES

1. Rees DC, Johnson E, Lewinson O. ABC transporters: the power to change. *Nat Rev Mol Cell Biol*. 2009;10:218-227.
2. Vasiliou V, Vasiliou K, Nebert DW. Human ATP-binding cassette (ABC) transporter family. *Hum Genomics*. 2009;3:281-290.
3. Srivastava A. Progressive familial intrahepatic cholestasis. *J Clin Exp Hepatol*. 2014;4:25-36.
4. Wang N, Lan D, Chen W, Matsuura F, Tall AR. ATP-binding cassette transporters G1 and G4 mediate cellular cholesterol efflux to high-density lipoproteins. *Proc Natl Acad Sci U S A*. 2004;101:9774-9779.
5. Mosser J, Douar AM, Sarde CO, et al. Putative X-linked adrenoleukodystrophy gene shares unexpected homology with ABC transporters. *Nature*. 1993;361:726-730.
6. Wiesinger C, Kunze M, Regelsberger G, Forss-Petter S, Berger J. Impaired very long-chain acyl-CoA  $\beta$ -oxidation in human X-linked adrenoleukodystrophy fibroblasts is a direct consequence of ABCD1 transporter dysfunction. *J Biol Chem*. 2013;288:19269-19279.
7. The metabolic basis of inherited disease. 6th edition. *Jpn J Hum Genet*. 1989;34:253.
8. Rommens JM, Iannuzzi MC, Kerem BS, et al. Identification of the cystic fibrosis gene: chromosome walking and jumping. *Science*. 1989;245:1059-1065.
9. Allikmets R, Singh N, Sun H, et al. A photoreceptor cell-specific ATP-binding transporter gene (ABCR) is mutated in recessive Stargardt macular dystrophy. *Nat Genet*. 1997;15:236-246.
10. Schaedler TA, Faust B, Shintre CA, et al. Structures and functions of mitochondrial ABC transporters. *Biochem Soc Trans*. 2015;43:943-951.
11. Begley DJ. ABC transporters and the blood-brain barrier. *Curr Pharm Des*. 2004;10:1295-1312.
12. Thomas C, Tampe R. Structural and mechanistic principles of ABC transporters. *Annu Rev Biochem*. 2020;89:605-636.
13. Shvarev D, Janulienė D, Moeller A. Frozen motion: how cryo-EM changes the way we look at ABC transporters. *Trends Biochem Sci*. 2021;47:136-148.
14. Locher KP. Mechanistic diversity in ATP-binding cassette (ABC) transporters. *Nat Struct Mol Biol*. 2016;23:487-493.
15. Verhalen B, Dastvan R, Thangapandian S, et al. Energy transduction and alternating access of the mammalian ABC transporter P-glycoprotein. *Nature*. 2017;543:738-741.
16. Chaptal V, Zampieri V, Wiseman B, et al. Substrate-bound and substrate-free outward-facing structures of a multidrug ABC exporter. *Sci Adv*. 2022;8:eabg9215.
17. Hofmann S, Janulienė D, Mehdipour AR, et al. Conformation space of a heterodimeric ABC exporter under turnover conditions. *Nature*. 2019;571:580-583.
18. Xie T, Zhang Z, Fang Q, Du B, Gong X. Structural basis of substrate recognition and translocation by human ABCA4. *Nat Commun*. 2021;12:3853.
19. Scortecci JF, Molday LL, Curtis SB, et al. Cryo-EM structures of the ABCA4 importer reveal mechanisms underlying substrate binding and Stargardt disease. *Nat Commun*. 2021;12:5902.
20. Qian H, Zhao X, Cao P, Lei J, Yan N, Gong X. Structure of the human lipid exporter ABCA1. *Cell*. 2017;169:1228-1239.e10.
21. Sun Y, Li X. Cholesterol efflux mechanism revealed by structural analysis of human ABCA1 conformational states. *Nat Cardiovasc Res*. 2022;1:238-245.
22. Khera AV, Cuchel M, de la Llera-Moya M, et al. Cholesterol efflux capacity, high-density lipoprotein function, and atherosclerosis. *N Engl J Med*. 2011;364:127-135.
23. Quazi F, Lenevich S, Molday RS. ABCA4 is an N-retinylidene-phosphatidylethanolamine and phosphatidylethanolamine importer. *Nat Commun*. 2012;3:925.
24. Mata NL, Weng J, Travis GH. Biosynthesis of a major lipofuscin fluorophore in mice and humans with ABCR-mediated retinal and macular degeneration. *Proc Natl Acad Sci U S A*. 2000;97:7154-7159.
25. Weng J, Mata NL, Azarian SM, Tzekov RT, Birch DG, Travis GH. Insights into the function of rim protein in photoreceptors and etiology of Stargardt's disease from the phenotype in abcr knockout mice. *Cell*. 1999;98:13-23.
26. Sparrow JR, Wu Y, Kim CY, Zhou J. Phospholipid meets all-trans-retinal: the making of RPE bisretinoids. *J Lipid Res*. 2010;51:247-261.
27. Pollock NL, Callaghan R. The lipid translocase, ABCA4: seeing is believing. *FEBS J*. 2011;278:3204-3214.
28. Molday RS, Zhong M, Quazi F. The role of the photoreceptor ABC transporter ABCA4 in lipid transport and Stargardt macular degeneration. *Biochem Biophys Acta*. 2009;1791:573-583.

29. Allikmets R, Shroyer NF, Singh N, et al. Mutation of the Stargardt disease gene (ABCR) in age-related macular degeneration. *Science*. 1997;277:1805-1807.
30. Martínez-Mir A, Paloma E, Allikmets R, et al. Retinitis pigmentosa caused by a homozygous mutation in the Stargardt disease gene ABCR. *Nat Genet*. 1998;18:11-12.
31. Cremers FPM, van de Pol DJ, van Driel M, et al. Autosomal recessive retinitis pigmentosa and cone-rod dystrophy caused by splice site mutations in the Stargardt's disease gene ABCR. *Hum Mol Genet*. 1998;7:355-362.
32. Liu FY, Lee J, Chen J. Molecular structures of the eukaryotic retinal importer ABCA4. *Elife*. 2021;10:e63524.
33. Kennedy MA, Barrera GC, Nakamura K, et al. ABCG1 has a critical role in mediating cholesterol efflux to HDL and preventing cellular lipid accumulation. *Cell Metab*. 2005;1:121-131.
34. Out R, Hoekstra M, Hildebrand RB, et al. Macrophage ABCG1 deletion disrupts lipid homeostasis in alveolar macrophages and moderately influences atherosclerotic lesion development in LDL receptor-deficient mice. *Arterioscler Thromb Vasc Biol*. 2006;26:2295-2300.
35. Wang N, Ranalletta M, Matsuura F, Peng F, Tall Alan R. LXR-induced redistribution of ABCG1 to plasma membrane in macrophages enhances cholesterol mass efflux to HDL. *Arterioscler Thromb Vasc Biol*. 2006;26:1310-1316.
36. Sun Y, Wang J, Long T, et al. Molecular basis of cholesterol efflux via ABCG subfamily transporters. *Proc Natl Acad Sci U S A*. 2021;118(34):e2110483118.
37. Skarda L, Kowal J, Locher KP. Structure of the human cholesterol transporter ABCG1. *J Mol Biol*. 2021;433:167218.
38. Xu D, Li Y, Yang F, et al. Structure and transport mechanism of the human cholesterol transporter ABCG1. *Cell Rep*. 2022;38:110298.
39. Fetsch PA, Abati A, Litman T, et al. Localization of the ABCG2 mitoxantrone resistance-associated protein in normal tissues. *Cancer Lett*. 2006;235:84-92.
40. Taylor NMI, Manolaridis I, Jackson SM, Kowal J, Stahlberg H, Locher KP. Structure of the human multidrug transporter ABCG2. *Nature*. 2017;546:504-509.
41. Jackson SM, Manolaridis I, Kowal J, et al. Structural basis of small-molecule inhibition of human multidrug transporter ABCG2. *Nat Struct Mol Biol*. 2018;25:333-340.
42. Manolaridis I, Jackson SM, Taylor NMI, Kowal J, Stahlberg H, Locher KP. Cryo-EM structures of a human ABCG2 mutant trapped in ATP-bound and substrate-bound states. *Nature*. 2018;563:426-430.
43. Orlando BJ, Liao M. ABCG2 transports anticancer drugs via a closed-to-open switch. *Nat Commun*. 2020;11:2264.
44. Kowal J, Ni D, Jackson SM, Manolaridis I, Stahlberg H, Locher KP. Structural basis of drug recognition by the multidrug transporter ABCG2. *J Mol Biol*. 2021;433:166980.
45. Yu Q, Ni D, Kowal J, et al. Structures of ABCG2 under turnover conditions reveal a key step in the drug transport mechanism. *Nat Commun*. 2021;12:4376.
46. Khunweeraphong N, Stockner T, Kuchler K. The structure of the human ABC transporter ABCG2 reveals a novel mechanism for drug extrusion. *Sci Rep*. 2017;7:13767.
47. Graf GA, Yu L, Li WP, et al. ABCG5 and ABCG8 are obligate heterodimers for protein trafficking and biliary cholesterol excretion. *J Biol Chem*. 2003;278:48275-48282.
48. Lee JY, Kinch LN, Borek DM, et al. Crystal structure of the human sterol transporter ABCG5/ABCG8. *Nature*. 2016;533:561-564.
49. Zhang H, Huang CS, Yu X, et al. Cryo-EM structure of ABCG5/G8 in complex with modulating antibodies. *Commun Biol*. 2021;4:526.
50. Dean M, Rzhetsky A, Allikmets R. The human ATP-binding cassette (ABC) transporter superfamily. *Genome Res*. 2001;11:1156-1166.
51. Kamijo K, Taketani S, Yokota S, Osumi T, Hashimoto T. The 70-kDa peroxisomal membrane protein is a member of the Mdr (P-glycoprotein)-related ATP-binding protein superfamily. *J Biol Chem*. 1990;265:4534-4540.
52. Lombard-Platet G, Savary S, Sarde CO, Mandel JL, Chimini G. A close relative of the adrenoleukodystrophy (ALD) gene codes for a peroxisomal protein with a specific expression pattern. *Proc Natl Acad Sci U S A*. 1996;93:1265-1269.
53. Watkins PA, Gould SJ, Smith MA, et al. Altered expression of ALDP in X-linked adrenoleukodystrophy. *Am J Hum Genet*. 1995;57:292-301.
54. Coelho D, Kim JC, Miousse IR, et al. Mutations in ABCD4 cause a new inborn error of vitamin B12 metabolism. *Nat Genet*. 2012;44:1152-1155.
55. Halbach A, Lorenzen S, Landgraf C, Volkmer-Engert R, Erdmann R, Rottensteiner H. Function of the PEX19-binding site of human adrenoleukodystrophy protein as targeting motif in man and yeast. PMP targeting is evolutionarily conserved. *J Biol Chem*. 2005;280:21176-21182.
56. Kashiwayama Y, Asahina K, Shibata H, et al. Role of Pex19p in the targeting of PMP70 to peroxisome. *Biochim Biophys Acta*. 2005;1746:116-128.
57. Kawaguchi K, Okamoto T, Morita M, Imanaka T. Translocation of the ABC transporter ABCD4 from the endoplasmic reticulum to lysosomes requires the escort protein LMBD1. *Sci Rep*. 2016;6:30183.
58. van Roermund CW, Visser WF, IJlst L, et al. The human peroxisomal ABC half transporter ALDP functions as a homodimer and accepts acyl-CoA esters. *FASEB J*. 2008;22:4201-4208.
59. van Roermund CW, IJlst L, Wagemans T, Wanders RJ, Waterham HR. A role for the human peroxisomal half-transporter ABCD3 in the oxidation of dicarboxylic acids. *Biochim Biophys Acta*. 2014;1841:563-568.
60. Tawbeh A, Gondcaille C, Trompier D, Savary S. Peroxisomal ABC transporters: an update. *Int J Mol Sci*. 2021;22(11):6093.
61. van Roermund CW, Visser WF, IJlst L, Waterham HR, Wanders RJ. Differential substrate specificities of human ABCD1 and ABCD2 in peroxisomal fatty acid  $\beta$ -oxidation. *Biochim Biophys Acta*. 2011;1811:148-152.
62. Moser HW, Mahmood A, Raymond GV. X-linked adrenoleukodystrophy. *Nat Clin Pract Neurol*. 2007;3:140-151.
63. Morita M, Shimozawa N, Kashiwayama Y, Suzuki Y, Imanaka T. ABC subfamily D proteins and very long chain fatty acid metabolism as novel targets in adrenoleukodystrophy. *Curr Drug Targets*. 2011;12:694-706.
64. Genin EC, Geillon F, Gondcaille C, et al. Substrate specificity overlap and interaction between adrenoleukodystrophy protein (ALDP/ABCD1) and adrenoleukodystrophy-related protein (ALDRP/ABCD2). *J Biol Chem*. 2011;286:8075-8084.
65. Fourcade S, Ruiz M, Camps C, et al. A key role for the peroxisomal ABCD2 transporter in fatty acid homeostasis. *Am J Physiol Endocrinol Metab*. 2009;296:E211-E221.
66. Ferdinandusse S, Jimenez-Sanchez G, et al. A novel bile acid biosynthesis defect due to a deficiency of peroxisomal ABCD3. *Hum Mol Genet*. 2015;24:361-370.
67. Chen ZP, Xu D, Wang L, et al. Structural basis of substrate recognition and translocation by human very long-chain fatty acid transporter ABCD1. *Nat Commun*. 2022;13:3299.
68. de Marcos Lousa C, van Roermund CWT, Postis VLG, et al. Intrinsic acyl-CoA thioesterase activity of a peroxisomal ATP binding cassette transporter is required for transport and metabolism of fatty acids. *Proc Natl Acad Sci U S A*. 2013;110:1279-1284.
69. Kawaguchi K, Mukai E, Watanabe S, et al. Acyl-CoA thioesterase activity of peroxisomal ABC protein ABCD1 is required for the

- transport of very long-chain acyl-CoA into peroxisomes. *Sci Rep*. 2021;11:2192.
70. Kitai K, Kawaguchi K, Tomohiro T, Morita M, So T, Imanaka T. The lysosomal protein ABCD4 can transport vitamin B(12) across liposomal membranes in vitro. *J Biol Chem*. 2021;296:100654.
  71. Xu D, Feng Z, Hou WT, et al. Cryo-EM structure of human lysosomal cobalamin exporter ABCD4. *Cell Res*. 2019;29:1039-1041.
  72. Bendre AD, Peters PJ, Kumar J. Recent insights into the structure and function of mycobacterial membrane proteins facilitated by cryo-EM. *J Membr Biol*. 2021;254:321-341.
  73. Leier I, Jedlitschky G, Buchholz U, Cole SP, Deeley RG, Keppler D. The MRP gene encodes an ATP-dependent export pump for leukotriene C4 and structurally related conjugates. *J Biol Chem*. 1994;269:27807-27810.
  74. Klein I, Sarkadi B, Váradi A. An inventory of the human ABC proteins. *Biochim Biophys Acta*. 1999;1461:237-262.
  75. Coyle B, Kessler M, Sabnis DH, Kerr ID. ABCB1 in children's brain tumours. *Biochem Soc Trans*. 2015;43:1018-1022.
  76. Liu X. ABC family transporters. *Adv Exp Med Biol*. 2019;1141:13-100.
  77. Androlewicz MJ, Ortmann B, van Endert PM, Spies T, Cresswell P. Characteristics of peptide and major histocompatibility complex class I/beta 2-microglobulin binding to the transporters associated with antigen processing (TAP1 and TAP2). *Proc Natl Acad Sci U S A*. 1994;91:12716-12720.
  78. al-Hussaini A, Lone K, Bashir MS, et al. ATP8B1, ABCB11, and ABCB4 genes defects: novel mutations associated with cholestasis with different phenotypes and outcomes. *J Pediatr*. 2021;236:113-123.e2.
  79. Park HJ, Kim TH, Kim SW, et al. Functional characterization of ABCB4 mutations found in progressive familial intrahepatic cholestasis type 3. *Sci Rep*. 2016;6:26872.
  80. Guo Q, Grimmig T, Gonzalez G, et al. ATP-binding cassette member B5 (ABCB5) promotes tumor cell invasiveness in human colorectal cancer. *J Biol Chem*. 2018;293:11166-11178.
  81. Hou L, Zhang X, Jiao Y, et al. ATP binding cassette subfamily B member 9 (ABCB9) is a prognostic indicator of overall survival in ovarian cancer. *Medicine (Baltimore)*. 2019;98:e15698.
  82. Srinivasan V, Pierik AJ, Lill R. Crystal structures of nucleotide-free and glutathione-bound mitochondrial ABC transporter Atm1. *Science*. 2014;343:1137-1140.
  83. Kim Y, Chen J. Molecular structure of human P-glycoprotein in the ATP-bound, outward-facing conformation. *Science*. 2018;359:915-919.
  84. Alam A, Kowal J, Broude E, Roninson I, Locher KP. Structural insight into substrate and inhibitor discrimination by human P-glycoprotein. *Science*. 2019;363:753-756.
  85. Bankstahl JP, Bankstahl M, Römermann K, et al. Tariquidar and Elacridar are dose-dependently transported by P-glycoprotein and Bcrp at the blood-brain barrier: a small-animal positron emission tomography and in vitro study. *Drug Metab Dispos*. 2013;41:754-762.
  86. Nosol K, Romane K, Irobalieva RN, et al. Cryo-EM structures reveal distinct mechanisms of inhibition of the human multidrug transporter ABCB1. *Proc Natl Acad Sci U S A*. 2020;117:26245-26253.
  87. Wang L, Hou WT, Wang J, et al. Structures of human bile acid exporter ABCB11 reveal a transport mechanism facilitated by two tandem substrate-binding pockets. *Cell Res*. 2022;32:501-504.
  88. Zutz A, Gompf S, Schägger H, Tampé R. Mitochondrial ABC proteins in health and disease. *Biochim Biophys Acta*. 2009;1787:681-690.
  89. Keppler D, Kartenbeck J. The canalicular conjugate export pump encoded by the *cmrp/cmoat* gene. *Prog Liver Dis*. 1996;14:55-67.
  90. Reid G, Wielinga P, Zelcer N, et al. The human multidrug resistance protein MRP4 functions as a prostaglandin efflux transporter and is inhibited by nonsteroidal antiinflammatory drugs. *Proc Natl Acad Sci U S A*. 2003;100:9244-9249.
  91. Reid G, Wielinga P, Zelcer N, et al. Characterization of the transport of nucleoside analog drugs by the human multidrug resistance proteins MRP4 and MRP5. *Mol Pharmacol*. 2003;63:1094-1103.
  92. Cole SP, Deeley RG. Transport of glutathione and glutathione conjugates by MRP1. *Trends Pharmacol Sci*. 2006;27:438-446.
  93. Homolya L, Váradi A, Sarkadi B. Multidrug resistance-associated proteins: export pumps for conjugates with glutathione, glucuronate or sulfate. *Biofactors*. 2003;17:103-114.
  94. Loe DW, Almquist KC, Deeley RG, Cole SP. Multidrug resistance protein (MRP)-mediated transport of leukotriene C4 and chemotherapeutic agents in membrane vesicles. Demonstration of glutathione-dependent vincristine transport. *J Biol Chem*. 1996;271:9675-9682.
  95. Williams GC, Liu A, Knipp G, Sinko PJ. Direct evidence that saquinavir is transported by multidrug resistance-associated protein (MRP1) and canalicular multispecific organic anion transporter (MRP2). *Antimicrob Agents Chemother*. 2002;46:3456-3462.
  96. He SM, Li R, Kanwar JR, Zhou SF. Structural and functional properties of human multidrug resistance protein 1 (MRP1/ABCC1). *Curr Med Chem*. 2011;18:439-481.
  97. Paulusma CC, Kool M, Bosma PJ, et al. A mutation in the human canalicular multispecific organic anion transporter gene causes the Dubin-Johnson syndrome. *Hepatology*. 1997;25:1539-1542.
  98. König J, Rost D, Cui Y, Keppler D. Characterization of the human multidrug resistance protein isoform MRP3 localized to the basolateral hepatocyte membrane. *Hepatology*. 1999;29:1156-1163.
  99. Kool M, van der Linden M, de Haas M, et al. MRP3, an organic anion transporter able to transport anti-cancer drugs. *Proc Natl Acad Sci U S A*. 1999;96:6914-6919.
  100. Zelcer N, Saeki T, Reid G, Beijnen JH, Borst P. Characterization of drug transport by the human multidrug resistance protein 3 (ABCC3). *J Biol Chem*. 2001;276:46400-46407.
  101. van Aubele R, Smeets PHE, Peters JGP, Bindels RJM, Russel FGM. The MRP4/ABCC4 gene encodes a novel apical organic anion transporter in human kidney proximal tubules: putative efflux pump for urinary cAMP and cGMP. *J Am Soc Nephrol*. 2002;13:595-603.
  102. Chen ZS, Tiwari AK. Multidrug resistance proteins (MRPs/ABCCs) in cancer chemotherapy and genetic diseases. *FEBS J*. 2011;278:3226-3245.
  103. Johnson ZL, Chen J. ATP binding enables substrate release from multidrug resistance protein 1. *Cell*. 2018;172:81-89 e10.
  104. Johnson ZL, Chen J. Structural basis of substrate recognition by the multidrug resistance protein MRP1. *Cell*. 2017;168:1075-1085.e9.
  105. Elborn JS. Cystic fibrosis. *Lancet*. 2016;388:2519-2531.
  106. Bryan J, Crane A, Vila-Carriles WH, Babenko AP, Aguilar-Bryan L. Insulin secretagogues, sulfonylurea receptors and K(ATP) channels. *Curr Pharm Des*. 2005;11:2699-2716.
  107. Tucker SJ, Gribble FM, Zhao C, Trapp S, Ashcroft FM. Truncation of Kir6.2 produces ATP-sensitive K<sup>+</sup> channels in the absence of the sulphonylurea receptor. *Nature*. 1997;387:179-183.
  108. Aguilar-Bryan L, Clement JP IV, Gonzalez G, Kunjilwar K, Babenko A, Bryan J. Toward understanding the assembly and structure of KATP channels. *Physiol Rev*. 1998;78:227-245.
  109. Li N, Wu JX, Ding D, Cheng J, Gao N, Chen L. Structure of a pancreatic ATP-sensitive potassium channel. *Cell*. 2017;168:101-110 e10.
  110. Nelson PT, Jicha GA, Wang WX, et al. ABCC9/SUR2 in the brain: implications for hippocampal sclerosis of aging and a potential therapeutic target. *Ageing Res Rev*. 2015;24:111-125.
  111. Liu F, Zhang Z, Csanady L, Gadsby DC, Chen J. Molecular structure of the human CFTR ion channel. *Cell*. 2017;169:85-95.e8.
  112. Zhang Z, Liu F, Chen J. Molecular structure of the ATP-bound, phosphorylated human CFTR. *Proc Natl Acad Sci U S A*. 2018;115:12757-12762.
  113. Liu F, Zhang Z, Levit A, et al. Structural identification of a hotspot on CFTR for potentiation. *Science*. 2019;364:1184-1188.



114. Bandler PE, Westlake CJ, Grant CE, Cole SP, Deeley RG. Identification of regions required for apical membrane localization of human multidrug resistance protein 2. *Mol Pharmacol.* 2008;74:9-19.
115. Grant CE, Gao M, DeGorter MK, Cole SP, Deeley RG. Structural determinants of substrate specificity differences between human multidrug resistance protein (MRP) 1 (ABCC1) and MRP3 (ABCC3). *Drug Metab Dispos.* 2008;36:2571-2581.
116. Chan KW, Zhang H, Logothetis DE. N-terminal transmembrane domain of the SUR controls trafficking and gating of Kir6 channel subunits. *EMBO J.* 2003;22:3833-3843.
117. Lee KPK, Chen J, MacKinnon R. Molecular structure of human KATP in complex with ATP and ADP. *Elife.* 2017;6:e32481.
118. Wu JX, Ding D, Wang M, Kang Y, Zeng X, Chen L. Ligand binding and conformational changes of SUR1 subunit in pancreatic ATP-sensitive potassium channels. *Protein Cell.* 2018;9:553-567.
119. Ding D, Wang M, Wu JX, Kang Y, Chen L. The structural basis for the binding of Repaglinide to the pancreatic KATP Channel. *Cell Rep.* 2019;27:1848-1857 e4.
120. Bruggemann EP, Currier SJ, Gottesman MM, Pastan I. Characterization of the azidopine and vinblastine binding site of P-glycoprotein. *J Biol Chem.* 1992;267:21020-21026.
121. Jumper J, Evans R, Pritzel A, et al. Highly accurate protein structure prediction with AlphaFold. *Nature.* 2021;596(7873):583-589.
122. Varadi M, Anyango S, Deshpande M, et al. AlphaFold Protein Structure Database: massively expanding the structural coverage of protein-sequence space with high-accuracy models. *Nucleic Acids Res.* 2022;50(D1):D439-D444.
123. Oldham ML, Grigorieff N, Chen J. Structure of the transporter associated with antigen processing trapped by herpes simplex virus. *Elife.* 2016;5:e21829.
124. Jin MS, Oldham ML, Zhang Q, Chen J. Crystal structure of the multidrug transporter P-glycoprotein from *Caenorhabditis elegans*. *Nature.* 2012;490:566-569.
125. Lang C, Meier Y, Stieger B, et al. Mutations and polymorphisms in the bile salt export pump and the multidrug resistance protein 3 associated with drug-induced liver injury. *Pharmacogenet Genomics.* 2007;17:47-60.
126. Higgins DG, Sharp PM. CLUSTAL: a package for performing multiple sequence alignment on a microcomputer. *Gene.* 1988;73:237-244.
127. Kumar S, Stecher G, Li M, Knyaz C, Tamura K. MEGA X: molecular evolutionary genetics analysis across computing platforms. *Mol Biol Evol.* 2018;35:1547-1549.
128. Xie T, Zhang Z, Yue J, Fang Q, Gong X. Cryo-EM structures of the human surfactant lipid transporter ABCA3. *Sci Adv.* 2022;8:eabn3727.
129. Uргаonkar S, Nosol K, Said AM, et al. Discovery and characterization of potent dual P-glycoprotein and CYP3A4 inhibitors: design, synthesis, Cryo-EM analysis, and biological evaluations. *J Med Chem.* 2022;65:191-216.
130. Olsen JA, Alam A, Kowal J, Stieger B, Locher KP. Structure of the human lipid exporter ABCB4 in a lipid environment. *Nat Struct Mol Biol.* 2020;27:62-70.
131. Nosol K, Bang-Sørensen R, Irobalieva RN, et al. Structures of ABCB4 provide insight into phosphatidylcholine translocation. *Proc Natl Acad Sci U S A.* 2021;118:e2106702118.
132. Wang C, Cao C, Wang N, Wang X, Wang X, Zhang XC. Cryo-electron microscopy structure of human ABCB6 transporter. *Protein Sci.* 2020;29:2363-2374.
133. Song G, Zhang S, Tian M, et al. Molecular insights into the human ABCB6 transporter. *Cell Discov.* 2021;7:55.
134. Li S, Ren Y, Lu X, Shen Y, Yang X. Cryo-EM structure of human ABCB8 transporter in nucleotide binding state. *Biochem Biophys Res Commun.* 2021;557:187-191.
135. Shintre CA, Pike ACW, Li Q, et al. Structures of ABCB10, a human ATP-binding cassette transporter in apo- and nucleotide-bound states. *Proc Natl Acad Sci U S A.* 2013;110:9710-9715.
136. Wang L, Hou WT, Chen L, et al. Cryo-EM structure of human bile salts exporter ABCB11. *Cell Res.* 2020;30:623-625.
137. Fiedorczuk K, Chen J. Mechanism of CFTR correction by type I folding correctors. *Cell.* 2022;185:158-168.e11.
138. Wang R, Qin Y, Li X. Structural basis of acyl-CoA transport across the peroxisomal membrane by human ABCD1. *Cell Res.* 2022;32:214-217.
139. Le LTM, Thompson JR, Dang PX, Bhandari J, Alam A. Structures of the human peroxisomal fatty acid transporter ABCD1 in a lipid environment. *Commun Biol.* 2022;5:7.

**How to cite this article:** Hou W-T, Xu D, Wang L, et al. Plastic structures for diverse substrates: A revisit of human ABC transporters. *Proteins.* 2022;1-17. doi:10.1002/prot.26406